Drug Development and Industrial Pharmacy, 32:39–52, 2006

ISSN: 0363-9045 print / 1520-5762 online
DOI: 10.1080/03639040500388037

Taylor & Francis
Taylor & Francis Group

Preparation of Theophylline-Hydroxypropylmethylcellulose Matrices Using Supercritical Antisolvent Precipitation: A Preliminary Study

M. Moneghini and B. Perissutti
Department of Pharmaceutical Sciences, University of Trieste, Trieste, Italy

I. Kikic, M. Grassi, and A. Cortesi
Department of Chemical, Environmental, and Raw Materials Engineering, Trieste, Italy

F. Princivalle
Department of Earth Sciences, Trieste, Italy

ABSTRACT Several controlled release systems of drugs have been elaborated using a supercritical fluid process. Indeed, recent techniques using a supercritical fluid as a solvent or as an antisolvent are considered to be useful alternatives to produce fine powders. In this preliminary study, the effect of Supercritical Anti Solvent process (SAS) on the release of theophylline from matrices manufactured with hydroxypropylmethylcellulose (HPMC) was investigated. Two grades of HPMC (HPMC E5 and K100) as carriers were considered in order to prepare a sustained delivery system for theophylline which was used as a model drug. The characterization of the drug before and after SAS treatment, and the coprecipitates with carriers, was performed by X-ray Diffraction (XRD) and Differential Scanning Calorimetry (DSC). The dissolution rate of theophylline, theophylline-coprecipitates, and matricial tablets prepared with coprecipitates were determined. The physical characterizations revealed a substantial correspondence of the drug solid state before and after supercritical fluid treatment while drug-polymer interactions in the SAS-coprecipitates were attested. The dissolution studies of the matrices prepared compressing the coprecipitated systems showed that the matrices based on HPMC K100 were able to promote a sustained release of the drug. Further, this advantageous dissolution performance was found to be substantially independent of the pH of the medium. The comparison with the matrices prepared with untreated substances demonstrated that matrices obtained with SAS technique can provide a slower theophylline release rate. A new mathematical model describing the in vitro dissolution kinetics was proposed and successfully tested on these systems.

KEYWORDS Supercritical antisolvent technique, Theophylline, Hydroxypropylmethylcellulose, Modeling, Physicochemical characterization

Address correspondence to Mariarosa Moneghini, Department of Pharmaceutical Sciences, University of Trieste, Piazzale Europa 1 I-34127, Trieste, Italy; Tel: +39 040 5583105; Fax: +39 040 52572; E-mail: moneghin@univ.trieste.it

INTRODUCTION

The use of hydrophilic polymers is currently the most used method in controlling the release of drugs in the formulation of oral pharmaceutical

dosage forms. Hydroxypropylmethylcellulose (HPMC) is a polymer frequently used in formulation of controlled release devices due to its ability to rapidly form a gel layer at the matrix periphery exposed to aqueous media (Mandal, 1995). The drug is released from the matrix mainly by diffusion through water filled pores, and hence, the internal morphology of the matrix, particle size, viscosity, and proportion of the HPMC can influence the release rate of drugs (Campos-Aldrete & Villafuerte-Robles, 1991). Changing the other formulation factors such as manufacture process can modify the drug release from the matrix (Vásquez et al., 1992). Besides the methods traditionally used to prepare the drug-HPMC blends before the direct compression of the matrix, consisting of co-grinding (Pina & Veiga, 2000) or kneading (Espinoza et al., 2000), in this work we processed the mixture using supercritical fluids (SCF), starting from previous experiences attesting the ability to form drug sustained release systems using SCF techniques (Debenedetti et al., 1993; Falk et al., 1997; Ghaderi et al., 2000; Kikic & Sist, 1998).

Initially applied to extraction and separation, SCF have received increased attention as suitable media, in general, for the elaboration of materials and, in particular, the formation of pharmaceutical fine powders or coprecipitates. The precipitation of hydrophilic or poorly soluble drugs, the preparation of dry protein powder, and the formulation of drug delivery systems have been investigated over 10 years using carbon dioxide (CO_2) as the supercritical solvent or antisolvent. In this work, the CO_2-supercritical effect on the preparation of theophylline-HPMC coprecipitates subsequently processed in matrices was studied, considering two different molecular weights of this cellulose derivative: HPMC E5 and K100. Among the various SCF technologies in consideration of the poor solubility of these polymers in supercritical CO_2, a Supercritical Anti Solvent (SAS) method was chosen.

This process involves the spraying of the solution composed of the solute and the organic solvent into a continuous supercritical phase co-currently flowing. The simultaneous dissolution of the SCF in the liquid droplet and the evaporation of the organic solvent towards the supercritical phase led to a supersaturation of the solute in the liquid phase and, thus, to its precipitation (Mueller & Fischer, 1989; Thiering et al., 2001).

Literature provides numerous pharmaceutical applications of such a precipitation technique: it is a promising alternative method to production of micro and nanoparticles of different polymers (Bleich et al., 1993; Chattopadhyay & Gupta, 2002), to modification of solid state properties of drugs like sulfathiazole and chlorpropamide (Yeo et al., 2003), and to micronization of poorly soluble active substances such as hydrocortisone (Steckel et al., 1997), rifampicin (Reverchon & Marco, 2002), and amoxicillin (Reverchon et al., 2003).

In this study, theophylline (THEO) was chosen as a water-soluble model drug since it is relatively soluble in supercritical CO_2 and, its precipitation is possible in a wide range of fluid-dynamic and operative conditions (Subra & Vega, 2003; Johannsen & Brunner, 1994). Further, literature reports that the SAS process is also suitable for processing supercritical CO_2-soluble compounds (Subra & Vega, 2003). After coprecipitation of THEO and HPMC, the collected solid particles were characterized by X-ray diffraction (XRD), Differential Scanning Calorimetry (DSC), and in vitro dissolution test in order to understand the effect of the SAS process on the solid-state and dissolution properties of the prepared binary systems. The influence on the drug release from HPMC matrices was also investigated analyzing the THEO release profile from tables prepared by direct compression of coprecipitates. This release profile was compared with tablets containing pure THEO and tablets containing untreated materials. Finally, a mathematical model taking into account both drug dissolution and diffusion through the matrix swollen part (gel layer) was proposed. The model reliability was proven by its ability to fit the experimental data well.

EXPERIMENTAL

Materials

Theophylline-reagent grade (THEO) was kindly donated by Zanchetta (Montecarlo-Lucca, Italy); HPMC E5 (Methocel E5) (E5) and HPMC K100 (K100 M Premium) (K100) both of EP grade were purchased from Eingenmann and Veronelli (Rho, Milano, Italy). All of the analytical grade solvents were provided by Carlo Erba (Milano, Italy). CO_2 (purity 99.9%) was supplied by SIAD (Trieste, Italy).

Methods

Sorption Experiments

In consideration of the low HPMC solubility in CO_2 (Broadbent et al., 1997), the CO_2 affinity for both polymers was determined carrying out sorption experiments. A microbalance (Battara, Trieste, Italy), with a sensitivity of 10^{-6} g, located inside of an air oven (Memmert ULE 500, Schwabach, Germany) was used to measure the CO_2 absorbed by the HPMC at constant temperature. The CO_2 was added to the sample and the pressure was increased by steps of 5 bar. The quantity of CO_2 sorbed was registered when the steady state was reached and maintained for almost 20 min. The value of CO_2 weight ratio (w CO_2) was then plotted as a function of the pressure.

SAS Method

On the basis of literature data (Kordikowski et al., 1995), volumetric expansions of methanol, ethanol, acetone, and 1:1 (w/w) dichloromethane/ethanol mixture were checked. The 1:1 dichloromethane/ethanol mixture was chosen as solvent for further SAS experiments, with both HPMC E5 and K100 being the best compromise between solubility and volumetric expansion (Kordikowski et al., 1995; Wade & Weller, 1994; Kumar & Banker, 1993).

A schematic diagram of the SAS equipment used in this study is illustrated in Fig. 1 The precipitator (AISI-316 steel, internal diameter of 50 mm and internal volume of 400 cm^3) was jacketed ensuring temperature to be kept within ±0.5°C. The sample solutions, kept at the precipitator temperature by an electric heat plate, was pumped (ConstaMetric ® 3200 P/F) to the top of the precipitator and then sprayed through a nozzle with a diameter of 100 μm. Liquid CO_2 was fed from the bottom of the precipitator by a high pressure pump (ISCO Model 260D). The outlet flow was then filtered (0.22 μm) to prevent precipitate losses and regulated by a heated metering valve (Whitey SS-21RS4).

Temperature and pressure values in the precipitator were measured by a Delta OHM thermometer (HD 9214, ±0.1°C) and a DRUCK pressure transducer (DPI 260, ±0.1 bar). The precipitator was filled with CO_2 to the experimental pressure; then the solution and CO_2

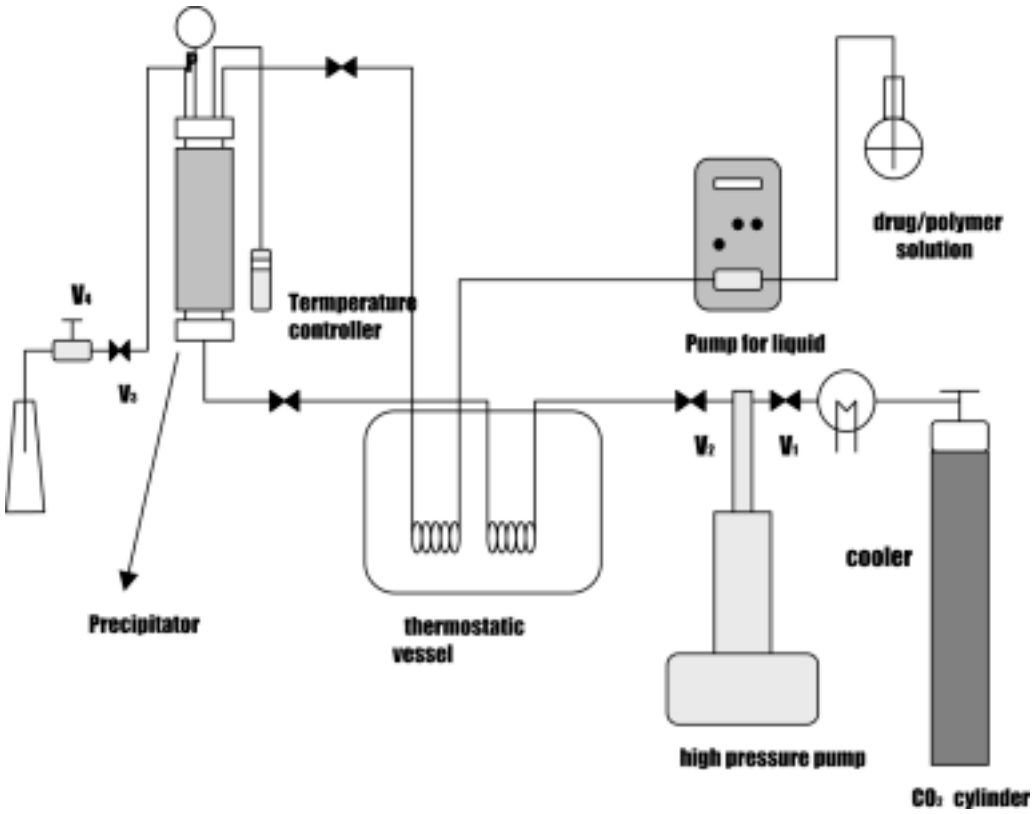

FIGURE 1 **Schematic Representation of the SAS Apparatus.**

were pumped to the reactor at constant flow. All experiments were performed using a flow rate of 8.0 mL/min and 0.40 mL/min for CO_2 and the solution, respectively. When all of the solution was added to the precipitator, only CO_2 was sent through the cell to strip the residual solvent from the precipitate that was washed with approximately 1000 mL of CO_2 before its collection.

For THEO, E5, K100, and for the binary systems, the experimental conditions were 40°C and 90 bar. Two theoretical THEO: HPMC weight ratios were considered to prepare coprecipitated binary systems (solid dispersions, SD): 1:1 and 1:9 w/w (effective drug: polymer ratio resulted to be 1:1 and 1:7.5, respectively, as discussed in the Results and Discussion section and reported in Table 1). In the case of 1:9, the sprayed solution was at the saturation point and this fact probably explained the discrepancy between the theoretical and the calculated value. The mean resulting yield was ranging about 90% w/w. The residual amount of solvents in the SAS-treated SD, determined by dynamic headspace chromatography, was found to be inferior to the USP limits for the considered solvents in pharmaceuticals.

For comparison, physical mixtures (PM) of the untreated components were prepared manually mixing in a mortar the untreated materials in the same proportions as the SD.

Preparation of the Matrices

The matrices (M) of 13 mm diameter were prepared by compression of 150 mg of powder (SD or PM) at a load of 3 tons for 60 sec in a manual tablet presser (Perkin Elmer, Norwalk, USA). The final tablets were approximately 1 mm thick. For comparison, 150 mg of untreated THEO were compressed in the same conditions (cpr THEO). Table 1 gives an overview of the compositions of the formulations evaluated during this study and their relative preparation methods.

Characterization of the Systems

Assay of the Total Drug Content

Known amounts of theophylline/polymer binary systems were added to ethanol and after 10 min of stirring the medium was filtered and diluted with ethanol to a concentration of about 20 μg/mL. The drug content was evaluated by spectrophotometry at 271 nm (Perkin Elmer, Spectrophotometer Mod. 552, Norwalk, USA) at which point the absorbance of the polymers is negligible. Calibration curve was obtained by plotting the absorbance of the standard drug solutions against the concentration. The percent drug content was compared to the calculated value. The experimental values were the average values of three replicates.

X-ray Powder Diffraction Studies

Samples were studied by means of XRD technique using a STOE D500 (Siemens, Munich, Germany) diffractometer with Cu Kα radiation, monochromatized by a secondary flat graphite crystal. The scanning angle ranges from 5–35° of 2θ, steps were of 0.05° of

TABLE 1 **Composition of the Formulation and Relative Preparation Methods**

Sample	Preparation method
THEO	Commercial sample
THEO-CO_2	Precipitated with SAS process
SD 1:1 THEO:E5 (w/w)	Coprecipitated with SAS process
SD 1:7.5 THEO:E5 (w/w)	Coprecipitated with SAS process
SD 1:1 THEO:K100 (w/w)	Coprecipitated with SAS process
PM 1:1 THEO:E5 (w/w)	Physical mixture
PM 1:7.5 THEO:E5 (w/w)	Physical mixture
PM 1:1 THEO:K100 (w/w)	Physical mixture
cpr THEO	Commercial sample compressed
M 1:1 (THEO:E5)-CO_2 (w/w)	Coprecipitated with SAS process and then compressed
M 1:1 THEO:E5 (w/w)	Physical mixture compressed
M 1:7.5 (THEO:E5)-CO_2 (w/w)	Coprecipitated with SAS process and then compressed
M 1:7.5 THEO:E5 (w/w)	Physical mixture compressed
M 1:1 (THEO:K100)-CO_2(w/w)	Coprecipitated with SAS process and then compressed
M 1:1 THEO:K100(w/w)	Physical mixture compressed

2θ, and the counting time was 1 sec/step. The current used was 20 mA and the voltage 40 kV.

Differential Scanning Calorimetry

Calorimetric analyses were performed with a DSC model TA 4000 (Mettler, Greifensee, Switzerland), equipped with a measuring cell DSC 20. Samples, containing about 2 mg of THEO, were placed in pierced aluminum pans and heated at a scanning rate of 10°C per min from 30–300°C under air atmosphere.

Determination of Drug Dissolution

The dissolution tests of pure THEO and binary systems (SD and PM) as a powder were performed according to the USP 28 paddle method: 100 rpm, 900 mL of dissolution medium, $T = 37 \pm 0.1$°C, sink conditions ($C < 0.2C_s$). For maintaining sink conditions, the dissolution tests of the matrices and the tablets of commercial THEO were performed using a modified USP 28 basket method (stirring rate of 100 rpm) employing a cylinder with a nominal capacity of 5000 mL instead of 1000 mL with the distance between the bottom of the basket and the bottom of the vessel being 50 mm.

In both cases, the composition of the dissolution media was 0.2 M NaCl/0.2 M HCl (pH 1.2) or 0.2 M KH_2PO/0.2 M NaOH (pH 7.4) according to USP 28. The aqueous solution was filtered and continuously pumped (Model SP 311, Velp Scientifica, Milano, Italy) to a flow cell in a spectrophotometer and absorbances were recorded at 271 nm. Polymers did not interfere with the UV (spectroscopic ultraviolet) analysis. Experimental points were the average of at least three replicates, and standard deviations did not exceed 5% of mean value.

Modeling of Drug Release Mechanism

Drug release kinetics from compacted systems made up by hydrophilic polymers is affected by many factors such as polymer swelling, polymer erosion, and drug dissolution characteristics besides drug/polymer ratio and the tablet geometric features (Conte et al., 1988; Colombo et al., 1999). Indeed, upon contact with the release fluids (water or physiological media), the polymer glassy dry state progressively transforms into a rubbery swollen one and, consequently, drug dissolution takes place. First, the release fluid (solvent) dissolves the drug amount present at tablet/release environment interface giving origin to a pronounced burst effect (Huang & Brazel, 2001) in the release profile; then it penetrates into the tablet according to the local porosity and to the polymer physical properties. As soon as the local penetrating concentration exceeds a threshold value, the polymeric chains begin to unfold so that the glassy/rubbery polymer transition occurs and a gel layer surrounding the tablet begins to appear (Kararli et al., 1990; Ju et al., 1995). The glassy/ rubbery transition enormously increases polymer chains mobility so that the drug can diffuse through the gel layer. Apart from the initial burst, the release kinetic is heavily ruled by the gel thickness, which in turn depends on the relative position of the eroding front (separating the release environment from the gel and moving outwards) and the swelling front (separating the dry glassy tablet core from the gel layer and moving inward). Additionally, in the case of sparingly soluble drugs, a third front, the diffusion front, can appear between the outer portion of the gel where the drug is completely dissolved, and the inner part, where the drug is not yet dissolved despite the rubbery state of the polymer (Colombo et al., 1996, 1999; Linder et al., 1996; Lee & Kim, 1991; Alhaique et al., 1993; Colombo, 1993; Tahara et al., 1995).

Although many powerful mathematical models were developed on this topic (Colombo et al., 2000), very often they are not so user friendly as they require numerical solutions. Accordingly, one aim of this work is to develop a new mathematical model of semi-empirical nature, but founded on reasonable assumptions, leading to an analytical solution.

The physical frame on which the present model relies is similar to that proposed by Higuchi et al. (1965) for the dissolution of a solid biphasic system. Accordingly, the tablet is seen as a uniform dispersion of two non-interacting solid phases whose dissolution kinetics depends on the respective dissolution constant and surface composition (the dissolution area available for each phase depends on the respective mass fraction). Our situation mainly differs from this frame for the fact that while phase 1 coincides with the solid drug, phase 2 is the polymer. Accordingly, upon contact with the external release environment fluid, phase 1 (drug) starts dissolving while phase 2 (polymer) starts swelling. Consequently, gel layer formation slows down drug delivery and release kinetics depends on the sum of two resistances in series, namely drug dissolution and drug

diffusion through the time dependent gel layer thickness. Gel layer thickness is the result of two counteracting phenomena: polymer swelling, causing an increase of gel thickness, and polymer erosion, determining a decrease of gel thickness. As a consequence, the time evolution of the gel layer thickness, proportional to gel resistance R to drug delivery, shows a peak connecting the initial increase with the final decrease. Obviously, the peak may be more or less pronounced and broad, and may appear in the early stage or after a very long time, so that sometimes (highly crosslinked or entangled gels) it never appears and a final plateau is encountered. Mathematically speaking, a whatever equation able to describe the above discussed gel thickness time evolution could be used to account for the gel layer resistance R. For the sake of simplicity, and in the light of our experimental data, two particular limiting situations are examined in this work. In the first case, gel layer formation is supposed to be slower than drug dissolution so that, at the beginning (time zero), gel layer resistance is zero (this corresponds to an infinite permeability value of gel layer being its thickness vanishing), and the only drug delivery resistance coincides with solid drug dissolution. In the second case, on the contrary, gel layer formation is supposed to be very fast (ideally, instantaneous) in comparison with drug dissolution so that gel layer thickness reaches a maximum value at the beginning and, then, it decreases due to erosion. These two limiting situations should apply for the case of gels made up by high molecular weight polymers (first case) and low molecular weight polymer (second case). Indeed, it seems reasonable that the formation of a gel constituted by a lower molecular weight polymer is more rapid than the formation of a chemically equal gel constituted by a higher molecular weight polymer. In addition, while in the second case (low polymer molecular weight) the erosion phenomena should exert an important role, in the first case (high molecular weight polymer) it should not be so important due to higher content of entanglements present in the gel. In order to translate this scenario in mathematical terms, the classical equation describing the dissolution of a solid drug in sink conditions is considered (Siekmann & Peppas, 2001):

$$\frac{dC_r}{dt} = -\frac{k_d A}{V_r} C_s \tag{1}$$

where t is time, C_r and C_s are drug concentration and solubility in the release environment, respectively, A is the release surface area, V_r is the release environment volume, and k_d is the dissolution constant. Now, we need to properly incorporate in Eq. 1 the effect of the gel layer resistance R and the tablet composition at the swelling front. So, bearing in mind that the global resistance to diffusion of a multi-layered membrane is given by the sum of the resistance of each layer (Siepmann & Peppas, 2001), and $1/k_d$ can be thought as the drug dissolution resistance, Eq. 1 can be re-written as:

$$\frac{dC_r}{dt} = -\frac{x_d A}{V_r} \frac{C_s}{\left(\frac{f}{k_d} + R\right)} \tag{2}$$

where x_d is the drug mass fraction at the swelling front and f is a parameter accounting for the fact that, due to gel presence, the drug dissolution constant k_d will be lower than that relative to pure solid drug dissolution (Flynn et al., 1974). x_d accounts for the fact that drug release also depends on the effective drug dissolution area at the swelling front.

Assuming that R is mainly affected by gel layer thickness, the first (slow gel layer formation; high molecular weight polymer) and second case (fast gel layer formation; low molecular weight polymer) can be represented, respectively, by the following equations (Colombo et al., 1996; Levich, 1962; Wan et al., 1995):

$$R = B\left(1 - \exp^{-bt}\right) \tag{3}$$

$$R = B\,e^{-bt} \tag{4}$$

where B and b are two model parameters to be determined by data fitting (obviously, gel permeability P is equal to $1/R$). While Eq. 3 implies an increase of gel resistance starting from zero up to a final plateau value ($R(t = \infty) = B$), Eq. 4 implies an instantaneous build up of gel resistance ($R(t = 0) = B$) followed by an exponential reduction due to erosion.

To complete the model, the time variation of the release area A has to be estimated. At this purpose, A is identified with the geometrical area competing to the diffusion front (in so doing it was assumed that crucial point for drug delivery is the area at the diffusion front rather than the tablet geometrical area, coinciding with the area of the eroding front) (Cappello et al.,

1994). Moreover, for the sake of simplicity, we assume that the ratio K between the height h and the radius R_a of the cylinder delimited by the diffusion front does not change with time and remains equal to that of the unswollen tablet. Accordingly, A modifies with time in the following way:

$$A = 2p(1+K)R_a^2(t) \tag{5}$$

In other words, the problem of the A time dependence is shifted on the R_a one, which can be determined by means of the following mass balance:

$$M_0 = V_r C_r(t) + pKR_a^3(t)C_0 \tag{6}$$

where M_0 is the drug amount initially contained in the tablet. In writing Eq. 6, we implicitly assume that the drug amount contained in the tablet portion delimited by the erosion and diffusion front is negligible. The rearrangement of Eq. 6 leads to:

$$R_a = \sqrt[3]{\frac{M_0 - V_r C_r(t)}{pKC_0}} \tag{7}$$

Inserting Eq. 7 into Eq. 5, we finally have:

$$A = \left(a - bC_r(t)\right)^{2/3} \tag{8}$$

$$a = \frac{(2p(1+K))^{3/2} M_0}{pKC_0} \qquad b = \frac{(2p(1+K))^{3/2} V_r}{pKC_0} \tag{9}$$

Now Eq. 8 can be embodied into Eq. 2 to give the final expression of the model differential form, whose solution is:

$$C_r^+ = \frac{C_r}{M_0/V_r} = 1 - \left(1 - \frac{2(1+K)x_d}{3M_0^{1/3}}\left(\frac{p}{K^2C_0^2}\right)^{1/3} F(t)\right)^3 \tag{10}$$

where for the first case (slow gel layer formation; high molecular weight polymer), $F(t)$ is given by:

$$F(t) = C_s\left[\frac{t}{B + 1/f k_d} + \frac{\ln\left(1 + B\left(1 - e^{-bt}\right) f k_d\right)}{\left(B + 1/f k_d\right) b}\right] \tag{11}$$

while it becomes:

$$F(t) = f k_d C_s\left[t + \ln\left(\frac{Be^{-bt} + 1/(k_d f)}{B + 1/f k_d}\right)\Big/ b\right] \tag{12}$$

for the second case (fast gel layer formation; low molecular weight polymer).

It is interesting to notice that, regardless $F(t)$ expression, Eq. 10 shows a flat behavior (its time derivatives vanishes, see Eqs. 2, 5 and 7) approaching the C_r^+ condition as required by the physic of the problem we are studying.

Finally, some considerations are needed about drug solubility C_s. Indeed, it may happen that upon dissolution the drug undergoes a phase transition reflecting into a modification of its solubility (Grassi et al., 2000) as happens in the case of anhydrous THEO that converts into the less soluble hydrate form (Nogami et al., 1969). Accordingly, a time dependent C_s should be considered. Although the model could account for this fact provided that some changes in its structure were considered, in this case we are not interested in this aspect as anhydrous THEO conversion into the hydrate form is very fast (De Smidt et al., 1986). Consequently, the identification of THEO solubility with hydrated form solubility implies a negligible error.

RESULTS AND DISCUSSION

Sorption Tests

Figure 2 reports the ratio between the amount of CO_2 sorbed by K100 and E5 (K100 w CO_2 and E5 w

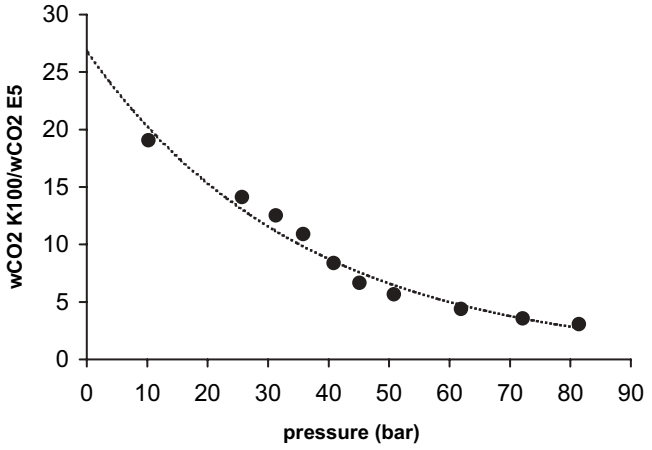

FIGURE 2 **Ratio Between the Amount of CO_2 Sorbed by HPMC K100 and E5 (40°C).**

CO_2) for each pressure. As it can be seen, the CO_2 sorption at 40°C resulted to be higher for K100 than E5, and the ratio between the K100 w CO_2 and E5 w CO_2 can be expressed by an exponential function. It can be concluded that the K100 showed a much higher affinity towards CO_2 compared to E5.

Precipitation Experiments

Supercritical antisolvent (SAS) runs, carried out at 40°C and 90 bar, gave in all cases a very light, voluminous powder as typical of the supercritical CO_2-precipitated samples. Co precipitated binary systems (SD) were prepared in two drug-to-polymer ratios. The analyses of drug content confirmed the theoretical value in the SD 1:1 whereas in the SD 1:9 THEO:E5 an effective drug-to-polymer weight ratio of 1:7.5 was found (Table 1). In the case of THEO:K100 only the 1:1 weight ratio was prepared. Attempts to prepare SD with a higher K100 content were unsuccessful, probably because the organic solvent acted as a cosolvent for the drug, increasing its solubility in CO_2 (Johannsen & Brunner, 1995).

Characterization of the Systems

XRD Analyses

The XRD peaks of the drug used in this study was assigned to the form II of anhydrous THEO as reported by Otsuka et al. (1990) (Fig. 3a). In particular, the reflections used for identification of anhydrous form II were at 12.7° and 26.6° of 2θ (Suzuki et al., 1989; Suihko et al., 1997). The X-ray diffraction patterns of pure drug treated by SCF were superimposable to that of anhydrous form II in terms of 2θ angles, and differences were noticed only in the relative intensities of the signals. This fact testified that the SAS treatment did not induce a polymorphic transition of the drug but lead to a certain diminution of drug crystallinity.

The diffractograms of the starting polymers, also depicted in Fig. 3a, showed a complete absence of signals and an elevated scattering phenomenon as typical of amorphous substances.

The diffractograms of the solid dispersions, presented in Fig. 3b, showed that the drug was still present in a crystalline state in all the drug-to-polymer ratios. Furthermore, a few peaks not attributable to any polymorphic forms of the drug nor to the carriers were detected, thus suggesting the existence of an

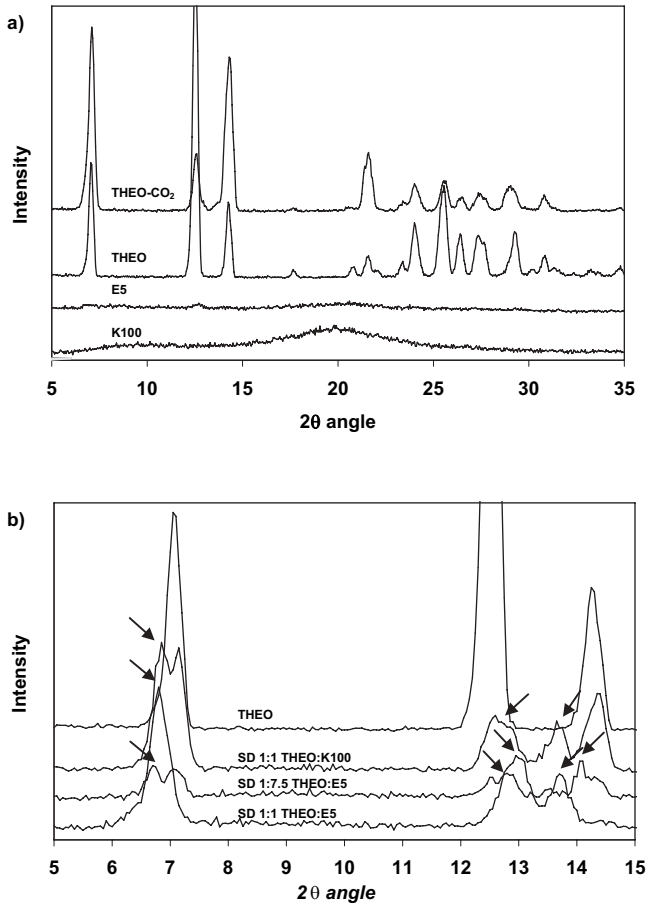

FIGURE 3 **XRD Patterns of the a) Single Components, and b) the SAS-treated Solid Dispersions Compared to the Original Drug.**

interaction between drug and carriers. In particular, three new signals were recorded at 6.85, 13, and 13.65 or 14 of 2θ (pointed by arrows). Moreover, a evident reduction of the intensity of the drug signals in the sample 1:7.5 THEO:E5 was noticed, that can be attributed both to the carrier dilution effect and to a partial loss of the drug crystallinity.

DSC Analyses

DSC thermograms of the SD containing THEO and E5, compared to the single components and to the corresponding physical mixtures of the untreated substances (PM), are shown in Fig. 4a.

The DSC traces of pure and treated drug showed a melting endotherm at 271.6°C (161.1 J/g), and at 270.7°C (141.0 J/g), respectively, indicating a certain diminution in THEO crystallinity after the supercritical process. There was no peak for the amorphous E5, apart from the broad endotherm between 35°C and 105°C, corresponding to its humidity.

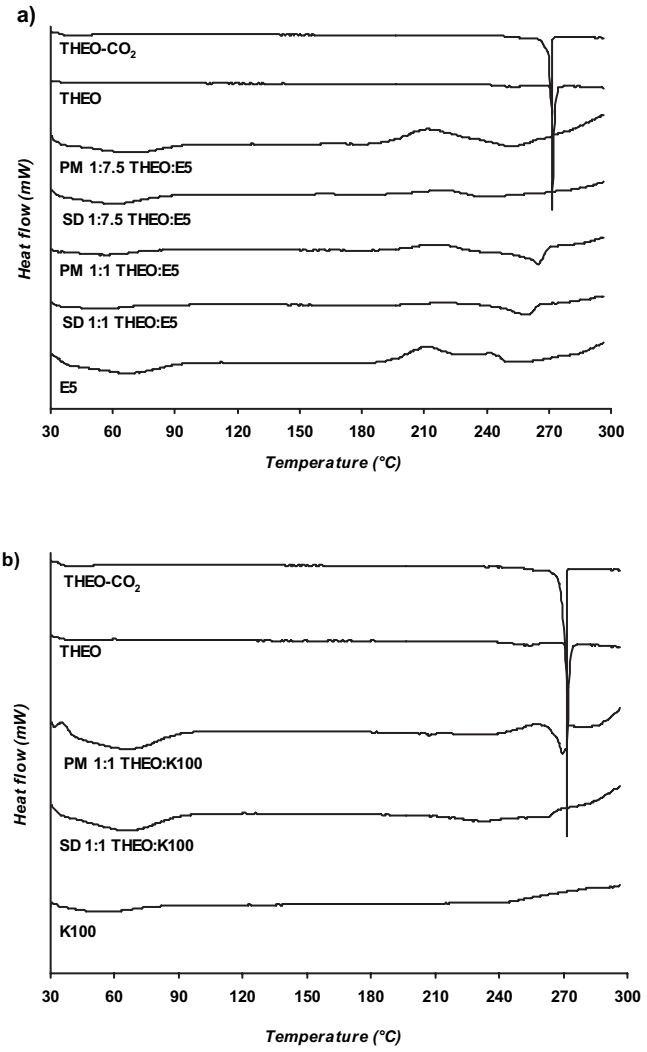

FIGURE 4 **DSC Traces of a) THEO:E5 Systems Compared to the Single Components and b) THEO:K100.**

In the 1:1 binary systems containing E5 (Fig. 4a), the thermal event due to the fusion of the drug was still present but a remarkable reduction of its enthalpy was detected and a shift of its melting point to 259.6°C and 264.2°C for the SAS-treated (SD) and physical mixture binary systems (PM), respectively. As the polymer content increased (1:7.5 THEO:E5), the fusion point diminished to about 180°C with a very broad endotherm and a dramatic reduction of the fusion enthalpy. These facts suggested the presence of interactions between drug and carrier at their solid state, in agreement to previous findings. All these DSC curves showed the decomposition of the polymer at temperatures higher than 200°C.

DSC traces of the SD 1:1 THEO:K100 and a corresponding PM compared to the single components are depicted in Fig. 4b. As previously reported (Suihko et al., 1997), the water loss by the pure K100 is significantly greater than that of E5 due to its higher molecular weight. The decomposition in this case started from about 250°C. Also, in the case of both THEO-K100 binary systems, a significant lowering of drug melting point and a reduction of the enthalpy related to this event were noticed.

Dissolution Tests

Figures 6 and 7 illustrate the in vitro dissolution profiles at pH 7.4 of the matrices prepared by direct compression of the THEO-E5 and THEO-K100 SD, respectively. The times required to dissolve 50% (t_{50}) and 90% (t_{90}) of the drug at both pH buffers were taken as a parameter for comparing the dissolution rate of starting THEO as a powder and as a tablet (cpr THEO) with its SD and M based on E5 or K100. These results are given in Table 2.

The profiles of the solid dispersions THEO-E5 and THEO K100 (data not shown) revealed the complete dissolution of the drug. Since both HPMC are hydrophilic polymers, the dissolution rate of the drug in these systems did not differ much from the pure drug.

On the other hand, the dissolution test of the THEO-E5 matrices showed that:

- the complete release of the drug in 60–85 min compared to 50 sec of pure drug as a powder and 40 min for the compressed form (cpr THEO);
- the release rate diminished with increased carrier content;
- pH of the medium did not influence the dissolution rate;
- the SAS treated systems gave a 30% slower release rate than PM systems, probably due the broader contact of the drug with the carriers and the subsequent change in the internal morphology of the matrices in comparison with those prepared with untreated substances.

The dissolution profiles of the THEO-K100 matrices indicated that:

- the use of a higher molecular weight HPMC lead to a remarkable reduction of the drug release rate achieving 90% of drug release after about 6 h;

TABLE 2 **Dissolution Parameters of the Samples**

	pH 1.2		pH 7.4	
Sample	$t_{50\%}$ (min)	$t_{90\%}$ (min)	$t_{50\%}$ (min)	$t_{90\%}$ (min)
THEO	0.37	0.89	0.35	0.86
SD 1:1 THEO:E5	0.80	2.50	0.70	2.34
SD 1:7.5 THEO:E5	0.63	2.34	0.63	2.34
SD 1:1 THEO:K100	0.92	2.50	1.17	3.08
cpr THEO	14.5	36	14.5	40
M 1:1 (THEO:E5)-CO_2	26	68	33	65
M 1:1 THEO:E5	18	36	28	51
M 1:7.5 (THEO:E5)-CO_2	41	75	40	85
M 1:7.5 THEO:E5	25	54	28	58
M 1:1 (THEO:K100)-CO_2	150	510	150	480
M 1:1 THEO:K100	110	360	110	350

- the treatment with SAS technique gave a further reduction of drug release rate: $t_{90\%}$ in 8 h (see M 1:1 (THEO:K100)-CO_2);
- also, in this case, the pH was not influent;
- the release rate of these matrices was ten times slower than THEO:E5 systems and this can be attributed to the higher viscosity of K100.

Modeling of Drug Release Mechanism

Due to the fact that medium pH does not affect drug release kinetics for both E5 and K100 matrices, data analysis will be focused on the pH = 7.4 case. Nevertheless, model fitting parameters referring to both the pH = 1.2 and 7.4 are reported in Table 3.

Figure 5 shows the comparison between model best fitting (solid lines) and the experimental data (symbols; for the sake of clarity, datum standard error, ranging from 1% to 5%, is not reported in this figure) referring to E5 matrices considering two different theophylline/E5 ratios (1:7.5, circles; 1:1 triangles) and two different preparation techniques (filled symbols, M (THEO:polymer)-CO_2; open symbols, M THEO:polymer). As it can be seen, a good data description can be noticed with the only exception, perhaps, of the beginning part of series M 1:7.5 (drug/polymer ratio 1:7.5, compression of PM). Nevertheless, it must be remembered that in this part of the

TABLE 3 **Each Tablet, Containing a Drug Amount Equal to M_0, Is Characterized by a Volume V_0, a Height/radius Ratio K, and a Drug Mass Fraction x_d**

pH 7.4	K(–)	M_0 (mg)	V_0 (cm^3)	x_d (–)	$F(t)$	B (min cm^{-1})	b (min^{-1})	f(–)
M 1:1 (THEO-E5)-CO_2	0.154	75	0.133	0.5	Eq. 11	13.1	0.030	1
M 1:1 THEO:E5	0.154	75	0.133	0.5	Eq. 11	16.3	0.083	1
M 1:7.5 (THEO-E5)-CO_2	0.154	17.7	0.133	0.117	Eq. 11	13.4	0.011	1
M 1:7.5 THEO-E5	0.154	17.7	0.133	0.117	Eq. 11	7.4	0.019	1
M 1:1 (THEO:K100)-CO_2	0.154	75	0.133	0.5	Eq. 9	71.3	0.038	0.49
M 1:1 THEO:K100	0.154	75	0.133	0.5	Eq. 9	50.0	0.051	0.52
pH 1.2	K(–)	M_0 (mg)	V_0 (cm^3)	x_d (–)	$F(t)$	B (min cm^{-1})	b (min^{-1})	f(–)
M 1:1 (THEO-E5)-CO_2	0.154	75	0.133	0.5	Eq. 11	5.5	15.6	1
M 1:1 THEO:E5	0.154	75	0.133	0.5	Eq. 11	7.6	0.220	1
M 1:7.5 (THEO-E5)-CO_2	0.154	17.7	0.133	0.117	Eq. 11	15.0	0.017	1
M 1:7.5 THEO-E5	0.154	17.7	0.133	0.117	Eq. 11	0.65	67.5	0.64
M 1:1 (THEO:K100)-CO_2	0.154	75	0.133	0.5	Eq. 9	72.2	0.028	0.34
M 1:1 THEO:K100	0.154	75	0.133	0.5	Eq. 9	50.7	0.052	0.55

B, b, and f are model fitting parameters.

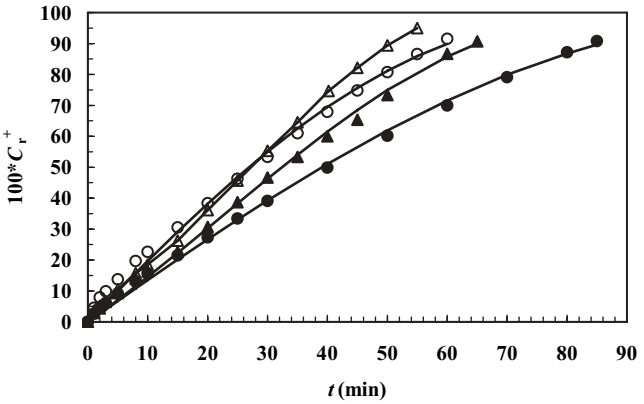

FIGURE 5 **Comparison Between the Model Best Fitting (Solid Lines) and Experimental Dissolution Data at pH 7.4 (Symbols) Referring to THEO-E5 Matrices: (●) M 1:7.5 (THEO:E5)-CO_2; (○) M 1:7.5 THEO:E5; (▲) M 1:1 (THEO:E5)-CO_2; and (?) M 1:1 THEO:E5.**

curve, where datum standard error is around 4%, model best fitting differs from experimental trend for a quantity smaller than the standard error. Accordingly, also in this case, model fitting is reasonable. Interestingly, while a satisfactory data fitting is achieved assuming that gel resistance decreases with time (Eqs. 4 and 12), the use of Eqs. 3 and 11, implying a gel resistance increase, does not provide a good description of experimental data. Ultimately, this proves that our model can supply information about gel layer thickness time evolution and that the choice of the proper equation typology ruling gel layer resistance variation is of paramount importance for what concerns a good data fitting. The fitting procedure is led assuming the physical and geometrical parameters reported in Table 3 and knowing (Grassi et al., 2001) that C_s = 12.5 mg/cm^3 and k_d = 0.188 cm/min. Figure 7 shows, for the four cases considered (THEO:E5 matrices), the matrix permeability trend P (=1/R) deduced from data fitting. Clearly it turns out that P increases with time, thus suggesting the idea that the main diffusional resistance is due to the rapid formation all around the matrix dry core of a layer more similar to a viscous aqueous polymer solution rather than to a structured (physical) hydrogel. Due to the liquid-like nature of this layer and the superimposed hydrodynamic conditions of the release environment, it becomes increasingly thinner with time due to polymer disentanglement and subsequent migration in the release environment. The low E5 molecular weight justifies the formation of a polymer solution rather than a physical gel, forming on condition that much longer polymeric chains are considered. Figure 7 also shows that P increase is higher for the 1:1 drug-polymer ratio (thin solid and dashed lines) and lower for the 1:7.5 drug-polymer ratio (thick solid and dashed lines). This is reasonable as lower polymer contents in the matrix result into a thinner, or lower polymer reach, surrounding layer. Moreover, Fig. 7 unequivocally shows that when CO_2 treatment is considered (solid thin and thick lines), permeability increase is remarkably lowered at both drug-polymer concentrations. Accordingly, it can be argued that coprecipitation favors very thin drug dispersion in the polymer, responsible for the formation of a more concentrated viscous layer. Indeed, the smaller the drug and polymer particles, the higher the polymer solubilization rate due to a reduced hindering action caused by the drug steric encumbrance and to a bigger dissolution surface per unit mass of polymer.

Figure 6 reports the comparison between model best fitting (solid lines) and the experimental data (symbols; for the sake of clarity, datum standard error, ranging from 1 to 5%, is not reported in this figure) referring to K100 matrices considering a drug-polymer ratio equal to 1:1 and two different preparation techniques (filled circles, M (THEO:polymer)-CO_2; circles, M THEO:polymer). The fitting procedure is led assuming the physical and geometrical parameters reported in Table 3 and knowing (Grassi et al., 2001) that C_s = 12.5 mg/cm^3 and k_d = 0.188 cm/min. In this case, a good agreement between experimental data and

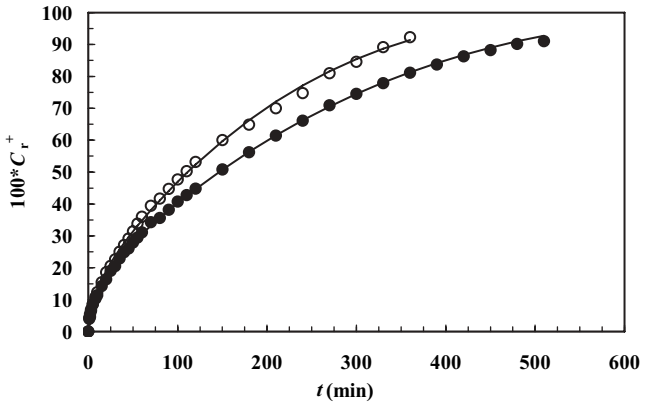

FIGURE 6 **Comparison Between the Model Best Fitting (Solid Lines) and Experimental Dissolution Data at pH 7.4 (Symbols) Referring to THEO-K100 Matrices: (●) M 1:1 (THEO:K100)-CO_2; (○) M 1:1 THEO:K100.**

model best fitting is achieved only assuming that gel resistance increases with time as reported in Eqs. 3 and 11. This turns out to be reasonable as the higher molecular weight polymer (K100) used makes more probable the formation of stronger chains entanglements responsible for the formation of a gel-like layer surrounding the matrix dry core. Accordingly, drug release rate is considerably slowed down in comparison with the E5 case (see Fig. 5 and 7). Indeed, the diffusional resistance of a gel-like structure is usually greater than that exerted by a solution. Conversely, the formation of a stronger gel can no longer be assumed instantaneous as in the E5 case (Fig. 7). Moreover, statistical analysis reveals that now *f* has to be considered as fitting parameters and its value is always lower than 1 (see Table 3). Again, the choice of a proper class of equation ruling gel resistance plays a fundamental role for a good data fitting. Figure 8 clearly shows that, also in this case, drug-polymer coprecipitation by means of CO_2 gives origin to smaller matrix permeability (greater resistance) (thick line) during the whole experimental time. Again, it can be argued that the thin drug-polymer dispersion favors the formation of a more connected (compact) gel structure. The fact that *P* decreases with time testimonies that gel thickness increases with time despite a sure erosion process promoted by the release environment mixing conditions and by the gel physical nature. This behavior can be easily seen also from an inspection of Table 3. Indeed, for both pH 7.4 and pH1.2 cases, the CO_2 treated systems show a statistically much bigger *B* value than that of the systems not treated with CO_2. This means that, in the CO2 treated systems, gel resistance is more important for drug release kinetics than for the untreated systems. Finally, regardless from pH conditions, an *f* comparison for CO_2 treated and not treated systems reveals the tendency of lower *f* values for treated systems. This would support the idea of a deep contact between drug and polymer–due to the CO_2 coprecipitation–that would delay drug dissolution.

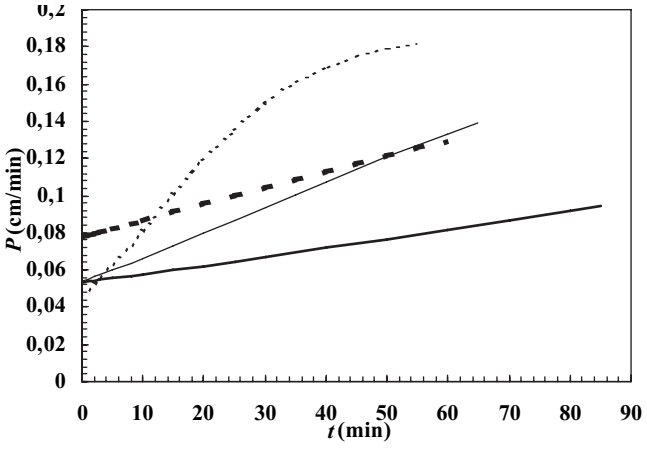

FIGURE 7 **Tablet Gel Layer Permeation (*P*) Time Dependence Coming from Model Data Fitting Performed on Data Shown in Fig. 5 (THEO:E5 matrices): (—) M 1:7.5 (THEO:E5)-CO_2; (– –) M 1:7.5 THEO:E5; (−) M 1:1 (THEO:E5)-CO_2; and (- -) M 1:1 THEO:E5.**

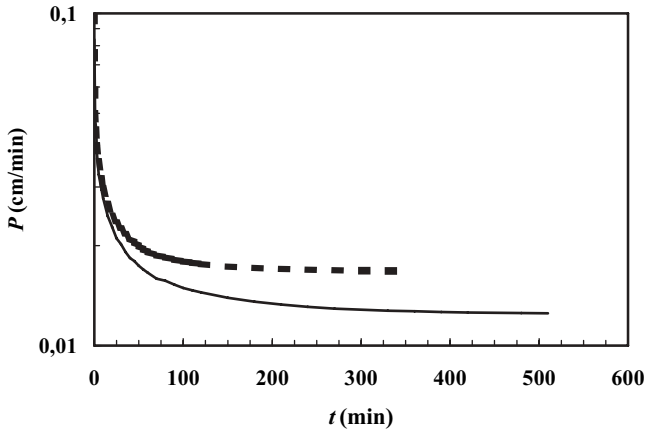

FIGURE 8 **Tablet Gel Layer Permeation (*P*) Time Dependence Coming from Model Data Fitting Performed on Data Shown in Fig. 6 (THEO:K100 matrices): (—) M 1:1 (THEO:K100)-CO_2; (– –) M 1:1 THEO:K100.**

CONCLUSIONS

From the above experimental evidence, it can be concluded that SAS process is a suitable technique for the preparation of drug/polymer solid dispersions. No evidence of a reorganization in a new polymorphic form of the drug was found, and crystalline drug was still detectable in all the binary systems prepared with SAS process. The physico-chemical characterization suggested the presence of some interactions between drug and carrier at their solid state. The formulation of the drug in K100, using the SAS process, and the subsequent processing in matrices gave a final sustained release device of the drug in which dissolution was found to be substantially unaffected from the pH of the medium. The comparison with the matrices prepared with untreated substances demonstrated a significantly slower drug release rate thanks to the broader contact of the drug with the carriers and the subsequent change in the internal morphology of the

matrices. It can be concluded that the proposed mathematical model, successfully applied also to other experimental data (Coviello et al., 1999; Grassi et al., 2004), gives a good description of the in vitro release kinetics of the considered systems, thus proving the model hypotheses reliability. Moreover, it allows for the release data interpretation in terms of matrix resistance (or permeability) and for comparing the relative importance of dissolution ($f * k_d$) and diffusion (R or P) through the layer surrounding the dry matrix core. An examination of Table 3 reveals that the diffusional resistance is larger than that associable to drug dissolution (that is around 5.3 min/cm) for the K100 systems, while it is comparable to that of drug dissolution for the E5 systems.

ACKNOWLEDGEMENTS

The authors wish to thank Regione Friuli Venezia Giulia (Italy) for financial support.

REFERENCES

Alhaique, F., Carafa, M., Riccieri, F. M., Santucci, E., & Touitou, E. (1993). Studies on the release behavior of polysaccharide matrix. *Pharmazie.*, *48*, 432–436.

Bleich, J., Muller, B. W., & Wassmus, W. (1993). Aerosol solvent extraction systems — A new microparticle production technique. *Int. J. Pharm.*, *97*, 111–117.

Broadbent, A., England, R., Staniford, J. N., & Crittenden, B. D. (1997). The potential of supercritical carbon dioxide as a solvent in the prediction of pharmaceutical products. *Proceedings of the 4th Italian Conference on Supercritical Fluids and Their Applications*, Capri, Italy.

Campos-Aldrete, M. E., & Villafuerte-Robles, L. (1991). Influence of viscosity grade and the particle size of HPMC on metronidazole release from matrix tablets. *Eur. J. Pharm. Biopharm.*, *43*, 173–178.

Cappello, B., Del Nobile, M. A., La Rotonda, M. I., Mensitieri, G., Miro, A., & Nicolais, L. (1994). Water soluble drug delivery systems based on a non-biological bioadhesive polymeric system. *Il Farmaco.*, *49*, 809–818.

Chattopadhyay, P., & Gupta, R. B. (2002). Supercritical CO_2 based production of magnetically responsive micro- and nanoparticles for drug targeting. *Ind. Eng. Chem. Res.*, *41*, 6049–6058.

Colombo, P. (1993). Swelling-controlled release in hydrogel matrices for oral route. *Adv. Drug Del. Rev.*, *11*, 37–57.

Colombo, P., Bettini, R., Castellani, P. L., Santi, P., & Peppas, N. A. (1999). Drug volume fraction profile in the gel phase and drug release kinetics in hydroxypropylmethyl cellulose matrices containing a soluble drug. *Eur. J. Pharm. Sci.*, *9*, 33–40.

Colombo, P., Bettini, R., & Peppas, N. A. (1999). Observation of swelling process and diffusion front position during swelling in hydroxypropyl methyl cellulose (HPMC) matrices containing a soluble drug. *J. Control. Rel.*, *61*, 83–91.

Colombo, P., Bettini, R., Santi, P., & Peppas, N. A. (2000). Swellable matrices for controlled drug delivery: gel-layer behaviour, mechanisms and optimal performance. *PSTT.*, *3*, 198–204.

Colombo, P., Bettini, R., Santi, P., De Ascentiis, A., & Peppas, NA. (1996). Analysis of the swelling and release mechanisms from drug delivery systems with emphasis on drug solubility and water transport. *J. Control. Rel.*, *39*, 231–237.

Conte, U., Colombo, P., Gazzaniga, A., Sangalli, M. E., & La Manna, A. (1988). Swelling-activated drug delivery system. *Biomaterials.*, *9*, 489–493.

Coviello, T., Grassi, M., Rambone, G., Santucci, E., Carafa, M., Murtas, E., Riccieri, F. M., & Alhaique, F. (1999). Novel hydrogel system from scleroglucan: synthesis and characterization. *J. Control. Rel.*, *60*, 367–378.

Debenedetti, P. G., Tom, J. W., Yeo, S. D., & Lim, G. B. (1993). Application of supercritical fluids for the production of sustained delivery devices. *J. Control. Rel.*, *24*, 27–44.

De Smidt, J. H., Fokkens, J. G., Grijseels, H., & Crommelin, D. J. A. (1986). Dissolution of theophylline monohydrate and anhydrous in buffer solutions. *J. Pharm. Sci.*, *75*, 497–501.

Espinoza, R., Hong, E., & Villafuerte, L. (2000). Influence of admixed citric acid on the release profile of pelanserin hydrochloride from HPMC matrix tablets. *Int. J. Pharm.*, *201*, 165–173.

Falk, R., Randolph, T. W., Meyer, J. D., Kelly, R.-M., & Manning, M. C. (1997). Controlled release of ionic compounds from poly (L-lactide) microspheres produced by precipitation with a compressed antisolvent. *J. Control. Rel.*, *44*, 77–85.

Flynn, G. L., Yalkowsky, S. H., & Roseman, T. J. (1974). Mass transport phenomena and models: theoretical concepts. *J. Pharm. Sci.*, *63*, 479–509.

Ghaderi, R., Artusson, P., & Carlfors, J. (2000). A new method for preparing biodegradable microparticles and entrapment of hydrocortisone in DL-PLG microparticles using supercritical fluids. *Eur. Pharm. Sci.*, *10*, 1–9.

Grassi, M., Colombo, I., & Lapasin, R. (2001). Experimental determination of the theophylline diffusion coefficient in swollen sodium-alginate membranes. *J. Control. Rel.*, *76*, 93–105.

Grassi, M., Zema, L., Sangalli, M. E., Giordano, F., & Gazzaniga, A. (2000). Modeling of drug release from high viscosity HPMC tablets. *Proceedings of the 27th International Symposium on Controlled Release of Bioactive Materials*, Paris, France, p. 6212.

Grassi, M., Zema, L., Sangalli, M. E., Maroni, A., Giordano, F., & Gazzaniga, A. (2004). Modelling of drug release from partially coated matrices made of a high viscosity HPMC. *Int. J. Pharm.*, *276*, 107–114.

Higuchi, W. I., Mir, N. A., & Desaj, S. J. (1965). Dissolution of polyphase mixtures. *J. Pharm. Sci.*, *54*, 1405–1410.

Huang, X., & Brazel, C. S. (2001). On the Importance and Mechanisms of Burst Release in Controlled Drug Delivery- A Review. *J. Control. Rel.*, *73*, 121–136.

Johannsen, M., & Brunner, G. (1995). Measurements of solubilities of xanthines in supercritical carbon dioxide + methanol. *J. Chem. Eng. Data.*, *40*, 431–434.

Johannsen, M., & Brunner, G. (1994). Solubilities of xanthines caffeine, theophylline and theobromine in supercritical carbon dioxide. *Fluid Phase Equilibria.*, *95*, 215–226.

Ju, R. T. C., Nixon, P. R., & Patel, M. V. (1995). Drug release from hydrophilic matrices. 1. New scaling laws for predicting polymer and drug release based on the polymer disentanglement concentration and the diffusion layer. *J. Pharm. Sci.*, *84*, 1455–1463.

Kararli, T. T., Hurlbut, J. B., & Needham, T. E. (1990). Glass-rubber transitions of cellulosic polymers by dynamic mechanical analysis. *J Pharm Sci.*, *79*, 845–848.

Kikic, I., & Sist, P. (1998). Application of supercritical fluids to pharmaceuticals: controlled drug release systems. *2nd NATO ASI Meeting on Supercritical Fluids, Kluwer Academic Publishers*, Antalya, Kemer, Turkey, July 12–24, Scientific Program and Abstracts of Presentations, p. 12.

Kordikowski, A., Schenk, A. P., Van Nielen, R. M., & Peters, C. J. (1995). Volume expansions and vapor-liquid equilibria of binary mixtures of a variety of polar solvents and certain near-critical solvents. *J. Supercrit Fluids.*, *8*, 205–216.

Kumar, V., & Banker, GS. (1993). Chemically-modified cellulose polymers. *Drug Dev. Ind. Pharm.*, *19*, 1–31.

Lee, I. P., & Kim, C. J. (1991). Probing the mechanism of drug release from hydrogels. *J. Control. Rel.*, *16*, 229–236.

Levich, V. G. (1962). *Physicochemical Hydrodynamics.* Englewood Cliffs: Prentice-Hall, 39–73.

Linder, W. D., Mockel, J. E., & Lippold, B. C. (1996). Controlled release of drugs from hydrocolloid embeddings. *Pharmazie,*, *51*, 263–272.

Mandal, T. K. (1995). The influence of binding solvents on drug release from hydroxypropylmethylcellulose tablets. *Drug Dev. Ind. Pharm.*, *11*, 1389–1397.

Mueller, B. W., Fischer, W. (1989). Verfahren zur Herstellung einer mindestens einen Wirkstoff und einen Träger umfassenden Zubereitung. German Patent Appl. No. DE 3744329 A1.

Nogami, H., Nagai, T., & Youtsuyanagi, T. (1969). Dissolution phenomena of organic medicinals involving simultaneous phase changes. *Chem. Pharm. Bull.*, *17*, 499–509.

Otsuka, M., Kaneniwa, K., Kawakami, K., & Umezawa, O. (1990). Effect of surface characteristics of theophylline anhydrate powder on hygroscopic stability. *J Pharm Pharmacol.*, *42*, 606–610.

Pina, M. E., & Veiga, F. (2000). The influence of diluent on the release of theophylline from hydrophilic matrix tablets. *Drug Dev. Ind. Pharm.*, *26*, 1125–1128.

Reverchon, E., De Marco, I., Caputo, G., & Della Porta, G. J. (2003). Pilot Scale micronization of amoxicillin by supercritical antisolvent precipitation. *J. Supercrit. Fluids*, *26*, 143–154.

Reverchon, E., De Marco, I., & Della Porta, G. (2002). Rifampicin microparticles production by supercritical antisolvent precipitation. *Int. J. Pharm.*, *243*, 83–91.

Siekmann, J., & Peppas, N. A. (2001). Modeling of drug release from delivery systems based on hydroxypropyl methylcellulose (HPMC). *Adv. Drug Del. Rev.*, *48*, 139–157.

Steckel, H., Thies, J., & Müller, B. W. (1997). Micronizing of steroids for pulmonary delivery by supercritical carbon dioxide. *Int. J. Pharm.*, *152*, 99–110.

Subra, P., & Vega, A. (2003). Crystallization in CO_2 medium: from phase equilibria to products. *Proceedings of the 6th International Symposium on Supercritical Fluids*, Brunner, G., Kikic, I., Perrut, M., Eds.; Versailles, France.

Suihko, E., Ketolainen, J., Poso, A., Ahlgren, M., Gynther, J., & Paronen, P. (1997). Dehydration of theophylline monohydrate—a two step process. *Int. J. Pharm.*, *158*, 7–55.

Suzuki, E., Shihomura, K., & Sekiguchi, K. (1989). Thermo-chemical study of theophylline and its hydrate. *Chem. Pharm. Bull.*, *37*, 493–497.

Tahara, K., Yamamoto, K., & Nishihata, T. (1995). Overall mechanism behind matrix sustained release (SR) tablets prepared with hydroxypropyl methylcellulose. *J. Control. Rel.*, *35*, 59–66.

Thiering, R., Deghani, F., & Foster, N. R. (2001). Current issue relating to anti-solvent micronization techniques and their extension to industrial scales. *J. Supercrit Fluids.*, *21*, 159–177.

Vásquez, M. J., Pérez-Marcos, B., Gòmez-Amoza, J. L., Martinez-Poacheco, R., Souto, C., & Concheiro, A. (1992). Influence of technological variables on release of drugs from hydrophilic matrices. *Drug Dev. Ind. Pharm.*, *18*, 1355–1375.

Wade, A., & Weller, P. J. (1994). *Handbook of Pharmaceutical Excipients*, (2nd Ed.). Washington and London: The American Pharmaceutical Association and the Pharmaceutical Society of Great Britain, 229–232.

Wan, L. S. C., Heng, P. W. S., & Wong, L. F. (1995). Matrix swelling: a simple model describing extent of swelling HPMC matrices. *Int. J. Pharm.*, *116*, 159–168.

Yeo, S. D., Kim, m S., & Lee, J. C. (2003). Recrystallization of sulfathiazole and chlorpropamide using the supercritical fluid antisolvent process. *J. Supercrit. Fluids*, *25*, 143–154.